Immunity, Vol. 8, 635–645, May, 1998, Copyright ©1998 by Cell Press

CD19 as a Membrane-Anchored Adaptor Protein of B Lymphocytes: Costimulation of Lipid and Protein Kinases by Recruitment of Vav

Lorraine M. O'Rourke,* Reuben Tooze,*
Martin Turner,‡§ David M. Sandoval,† Robert H. Carter,†
Victor L. J. Tybulewicz,‡ and Douglas T. Fearon*‖
*Wellcome Trust Immunology Unit
Department of Medicine
University of Cambridge School of Clinical Medicine
Cambridge CB2 2SP
United Kingdom
†Departments of Medicine and Microbiology
University of Alabama, Birmingham
Birmingham Veterans Affairs Medical Center
Birmingham, Alabama 35294
‡National Institute for Medical Research
The Ridgeway
London NW7 1AA
United Kingdom

Summary

CD19 is a coreceptor that amplifies signaling by membrane immunoglobulin (mIg) to promote responses of the B lymphocyte to T-dependent antigens. Vav is a guanine nucleotide exchange factor for the Rho, Rac, Cdc42 family of small GTPases. We found that coligating mIg and CD19 causes a synergistic increase in the tyrosine phosphorylation of CD19. Phosphorylated tyrosine-391 of CD19 binds Vav to mediate a sustained increase in intracellular Ca^{2+} concentration. This response correlates with activation by the CD19–Vav complex of phosphatidylinositol 4-phosphate 5-kinase for the synthesis of phosphatidylinositol 4,5-bisphosphate. Interaction of CD19 with Vav also mediates the synergistic activation of the mitogen-activated protein kinase JNK. Therefore, CD19 is a membrane adaptor protein that recruits Vav for the activation of lipid and protein kinases.

Introduction

CD19 is an essential coreceptor for membrane immunoglobulin (mIg), the antigen receptor of B lymphocytes. It is required for the formation of germinal centers and the normal production of antibody in response to T-dependent antigens; its deletion impairs and its overexpression augments these responses (Engel et al., 1995; Rickert et al., 1995; Sato et al., 1995). Through its association with the complement receptor, CD21, CD19 also links activation of the B lymphocyte to innate immune recognition of antigen. The potential of the CD19–CD21 complex for positively regulating immune responses is exemplified by the large increment in immunogenicity achieved by tagging antigen with C3d, the ligand for CD21 (Dempsey et al., 1996). CD19 also promotes the development and maintenance of the B-1 subset of B lymphocytes (Engel et al., 1995; Rickert et al., 1995; Krop et al., 1996), which expresses a distinct *V* gene repertoire, and it may regulate the expression of the *Rag-1* and *Rag-2* genes during B lymphocyte development (Billips et al., 1995).

The CD19–CD21 complex achieves these biological responses by synergistically enhancing signaling through mIg. Coligating CD19 or CD21 to mIg lowers the number of mIg required for inducing increases in intracellular Ca^{2+} concentration ($[Ca^{2+}]_i$) (Carter et al., 1991; Dempsey et al., 1996) and the proliferation of B lymphocytes (Carter and Fearon, 1992). The costimulatory effect of CD19 on $[Ca^{2+}]_i$ is associated with the enhanced generation of inositol 1,4,5-trisphosphate [$I(1,4,5)P_3$]; ligating CD19 alone also generates $I(1,4,5)P_3$, although the amounts are less. The mechanism for this function of CD19 is not known, but both the synergistic and the direct effects of CD19 on the production of $I(1,4,5)P_3$ occur without its altering the tyrosine phosphorylation of phospholipase C (PLC)–γ (Carter et al., 1991), suggesting that CD19 either enhances the efficiency of PLCγ or increases the availability of the substrate, phosphatidylinositol 4,5-bisphosphate [$PI(4,5)P_2$], which may become rate limiting for inositol lipid hydrolysis (Stephens et al., 1993), or does both.

CD19 also costimulates with mIg the mitogen-activated protein (MAP) kinases ERK2 (extracellular signal–regulated protein kinase 2), JNK/SAPK (c-Jun N-terminal kinase/stress-activated protein kinase), and p38 (Li et al., 1997; Tooze et al., 1997). Although ligating mIg or CD19 alone causes modest or no activation of these kinases, their coligation causes robust activation of all three, even at low levels of mIg cross-linking. Therefore, at least two general pathways of signaling by mIg are up-regulated by CD19: phosphatidylinositol metabolism, leading to elevated $[Ca^{2+}]_i$, and the MAP kinase cascades.

Vav and the Rho family of small guanosine triphosphatases (GTPases) offer a means by which these two apparently unrelated pathways may be stimulated in synchrony. Both Rho and Rac have been shown to interact with phosphatidylinositol 4-phosphate 5-kinase (PIP5K) (Chong et al., 1994; Hartwig et al., 1995; Tolias et al., 1995; Ren et al., 1996), which synthesizes $PI(4,5)P_2$ from phosphatidylinositol 4-phosphate (PI4P), and Rac initiates a MAP kinase pathway leading to JNK (Crespo et al., 1996). The activation of Rho and Rac requires their loading with guanosine triphosphate (GTP), and Vav is a guanine nucleotide exchange factor (GEF) for this family of GTPases that is expressed relatively exclusively in hematopoietic cells (Katzav et al., 1989; Crespo et al., 1997). This function of Vav is mediated by its Dbl homology domain and is positively regulated in vitro by tyrosine phosphorylation (Crespo et al., 1997; Han et al., 1997). In B and T lymphocytes, Vav is phosphorylated following ligation of the antigen receptors (Bustelo and Barbacid, 1992; Bustelo et al., 1992; Margolis et al., 1992). In addition, Vav is the only GEF that contains a

§Present address: The Babraham Institute, Babraham, Cambridge CB2 4AT, United Kingdom.
‖To whom correspondence should be addressed (e-mail: dtf1000@cus.cam.ac.uk).

Src homology (SH)–2 domain, suggesting that its function may also be regulated by interaction with proteins that have become tyrosine phosphorylated. Consistent with this possibility is the finding that in T lymphocytes, Vav-dependent functions are enhanced by coexpression of SLP-76, which, when tyrosine phosphorylated, serves as an adaptor for Vav (Reif et al., 1994; Wu et al., 1996; Raab et al., 1997).

Several observations have suggested that CD19 may recruit Vav to amplify B lymphocyte activation. CD19 is tyrosine phosphorylated when either it or mIg is ligated (Tuveson et al., 1993), and tyrosine-phosphorylated CD19 associates with Vav (Weng et al., 1994). Ligating CD19 alone induces tyrosine phosphorylation of Vav (Weng et al., 1994; Sato et al., 1997), and coligating CD19 with mIg causes synergistic phosphorylation of this GEF (Li et al., 1997). CD19 recruits phosphatidylinositol 3-kinase (PI3K), the product of which has been shown recently to promote the activation of Vav (Han et al., 1998). Mice lacking Vav (Tarakhovsky et al., 1995; Zhang et al., 1995) share with *CD19*$^{-/-}$ mice (Engel et al., 1995; Rickert et al., 1995) diminished numbers of B-1 cells. Accordingly, we have examined whether the interaction of CD19 with Vav mediates its role as a membrane-anchored adaptor protein that amplifies mIg signaling.

Results

Phosphorylating Tyrosine-391 of CD19 Mediates Binding of Vav

Ligating CD19 has been shown to induce an association with Vav (Weng et al., 1994), but the basis for the interaction is not known. We performed two sets of experiments to characterize the binding of Vav by CD19. Unstimulated murine splenic B lymphocytes, lymphocytes that had been activated by ligating either CD19 or mIg alone, and lymphocytes that had been activated by cross-linking CD19 to mIg were compared for the extent to which CD19 had become tyrosine phosphorylated and for the amount of Vav that was associated with CD19. In unstimulated B lymphocytes, there was no detectable tyrosine phosphorylation of CD19, and a relatively small amount of Vav coimmunoprecipitated with CD19 (Figure 1). Ligating CD19 alone slightly augmented both measurements, as did ligating mIg alone. However, the coligation of CD19 with mIg was found to have a synergistic effect, increasing both the tyrosine phosphorylation of CD19 and the association with Vav by approximately 10- to 20-fold when these measurements were corrected for recovery of CD19. The diminished recovery of CD19 in the detergent lysates of cells on which CD19 and mIg had been coligated was caused by tight association with detergent-insoluble cytoskeleton, and the high molecular form of phosphorylated CD19 was caused by ubiquitination of the receptor (L. M. O. and D. T. F., unpublished data).

We determined which of the nine potential phosphotyrosines (Y*) of the cytoplasmic domain of CD19 binds Vav. Streptavidin-agarose beads that had been coated with each of nine biotinylated 11-mer peptides containing Y* and flanking sequences corresponding to the

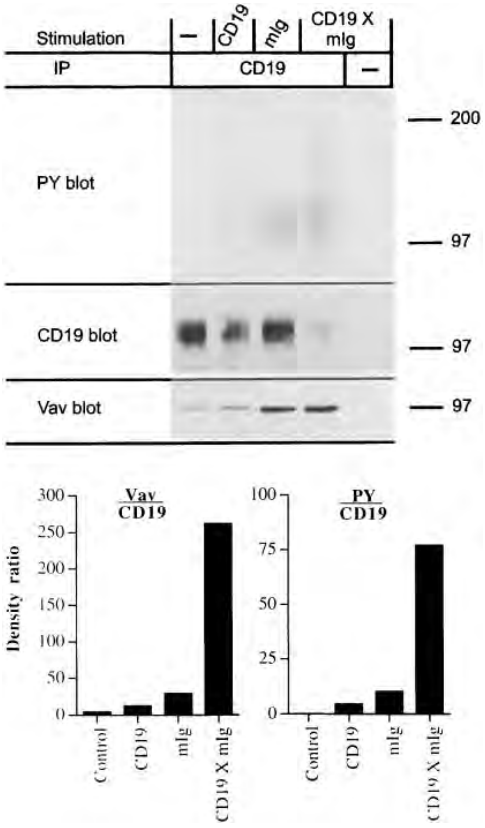

Figure 1. Enhancement of Vav Association with CD19 by Coligating CD19 to mIg

Splenic B cells were preincubated with the following biotinylated antibody fragments: control Fab (10 μg/ml), Fab anti-CD19 (10 μg/ml), Fab anti-κ (5 μg/ml), or Fab anti-κ and Fab anti-CD19 together. The cell-bound antibodies were cross-linked for 1 min by addition of avidin. The cells were lysed and CD19 was immunoprecipitated from cell lysates. The immunoprecipitated proteins were resolved by SDS-PAGE; transferred to nitrocellulose; and immunoblotted with monoclonal antibody to Vav, followed by enhanced chemiluminescence (ECL) with ^{125}I-labeled 4G10; and, after stripping, immunoblotted with rabbit antibody to the cytoplasmic domain of mouse CD19 followed by ECL. The relative amounts of tyrosine phosphorylated CD19, total recovered CD19, and Vav were quantitated using a Molecular Dynamics densitometer. The signals obtained by scanning the control immunoprecipitate were subtracted, and the ratios of Vav to total CD19 and of tyrosine phosphorylated CD19 to total CD19 were calculated.

cytoplasmic domain of human CD19 (Tedder and Isaacs, 1989) were incubated with replicate samples of lysates of Daudi human B lymphoblastoid cells. The agarose beads were washed, and bound proteins were eluted, resolved by sodium dodecyl sulfate (SDS)–polyacrylamide gel electrophoresis (PAGE), and immunoblotted with antibody to Vav. Only the peptide containing Y*391 bound Vav (Figure 2A), and only the phosphorylated form of this peptide adsorbed Vav from lysates of Daudi and Ramos human B lymphoblastoid cells and murine A20 cells (Figure 2B). These findings are consistent with earlier work predicting the specificity of the SH2 domain of Vav (Songyang et al., 1994).

To determine whether tyrosine-391 mediated the binding of Vav to CD19 in vivo, Daudi B lymphoblastoid cells

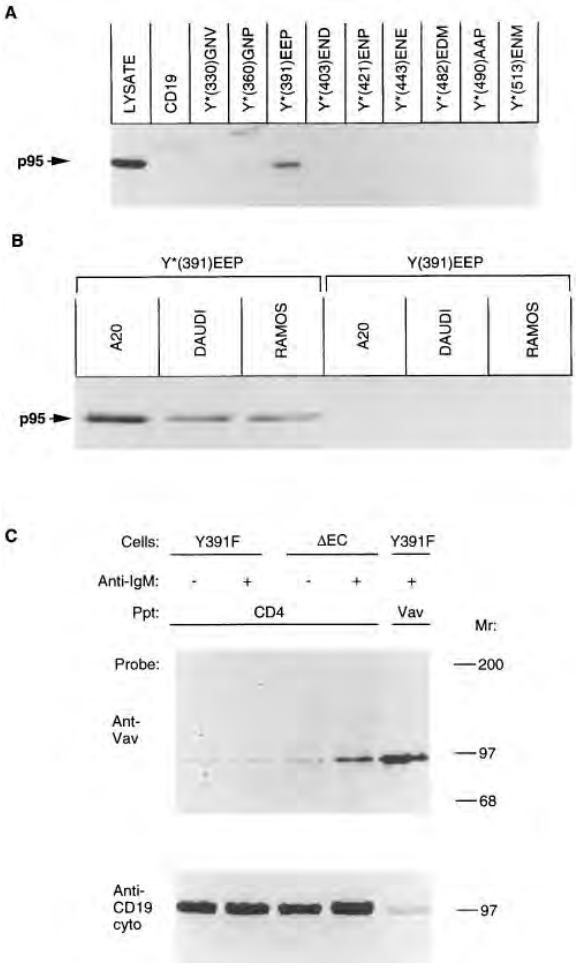

Figure 2. Interaction of Vav with Y*391 of CD19

(A) Streptavidin–agarose beads coated with 11-mer biotinylated phosphotyrosyl peptides corresponding to sequences in the cytoplasmic domain of human CD19: PQNQY*(330)GNVLSL, TAPSY*(360)GNPSSD, EGEGY*(391)EEPDSE, DSEFY*(403)ENDSNL, DGSGY*(421)ENPEDE, NAESY*(443)ENEDEL, GSQSY*(482)EDMRGI, RGILY*(490)AAPQLR, and DADSY*(513)ENMDNP, were incubated with lysates of Daudi B lymphoblastoid cells and adsorbed proteins were eluted, resolved by SDS-PAGE, transferred to nitrocellulose, and immunoblotted with antibody to Vav, followed by ECL. For comparison, a whole-cell lysate and a CD19 immunoprecipitate were immunoblotted with anti-Vav.

(B) Streptavidin–agarose beads coated with the phosphorylated and nonphosphorylated 11-mer peptides containing tyrosine-391 were incubated with lysates of Daudi, Ramos, and A20 cells. Bound proteins were eluted, resolved by SDS-PAGE, and immunoblotted with antibody to Vav.

(C) Replicate samples of Daudi B lymphoblastoid cells expressing the ΔEC (8×10^7 cells) or Y391F (4×10^7 cells) CD4/CD19 chimeric receptors were held in buffer or stimulated for 1 min with $F(ab')_2$ goat antibody to IgM. The chimeric receptors were immunoprecipitated from cell lysates by incubation with antibody to CD4; Vav was directly immunoprecipitated with anti-Vav from a lysate of 2×10^7 stimulated cells expressing Y391F. The immunoprecipitated proteins were resolved by SDS-PAGE, transferred to nitrocellulose, and immunoblotted with antibody to Vav, and, after stripping, with rabbit antibody to the cytoplasmic domain of CD19, followed by ECL.

were stably transfected with two chimeric CD4/CD19 receptors: ΔEC, in which the extracellular domain of CD19 was substituted with that of CD4 (Matsumoto et al., 1993), and the Y391F receptor, which had the additional modification of phenylalanine substituted for tyrosine-391 in the cytoplasmic domain (Li et al., 1997). The transfectants were untreated or were activated by cross-linking mIgM to induce the tyrosine phosphorylation of the chimeric receptors. These receptors and any associated proteins were immunoprecipitated from lysates with antibody to CD4, resolved by SDS-PAGE, and revealed by sequential immunoblotting with antibodies to Vav and the cytoplasmic domain of CD19, respectively. A small amount of Vav coprecipitated with the ΔEC and Y391F receptors from unstimulated cells; an interaction of Vav with chimeric CD4-CD19 that was independent of tyrosine-391 was also observed when Vav was primarily immunoprecipitated (Figure 2C). Ligating mIgM increased the amount of Vav coprecipitating with the ΔEC receptor, but not that with the Y391F receptor. Thus, the inducible interaction of CD19 with Vav requires tyrosine-391.

CD19, Vav, and the Maintenance of Elevated $[Ca^{2+}]_i$

The role of Vav in the elevation of $[Ca^{2+}]_i$ induced by either mIg or CD19 was examined in indo-1–loaded B cells from normal mice and from mice in which *Vav* had been interrupted by homologous recombination (Turner et al., 1997). The delayed and modest increase in $[Ca^{2+}]_i$ caused by ligating large numbers of CD19 alone on wild-type B lymphocytes was absent in $Vav^{-/-}$ B lymphocytes (Figure 3A). In contrast, and as previously reported (Tarakhovsky et al., 1995; Zhang et al., 1995), cross-linking mIg induced comparable increases in $[Ca^{2+}]_i$ in $Vav^{+/+}$ and $Vav^{-/-}$ B lymphocytes (Figure 3B). Coligating suboptimal numbers of CD19 and mIg led to a synergistic initial increase in $[Ca^{2+}]_i$ that did not require Vav and a sustained Ca^{2+} response that was dependent on Vav (Figures 3C and 3D). Therefore, Vav contributes to the regulation of $[Ca^{2+}]_i$ by CD19, especially the synergistic, long-term (≥10 min) elevation of $[Ca^{2+}]_i$.

CD19 Activates PIP5K via Vav

Taken together, the requirement for Vav to maintain elevated $[Ca^{2+}]_i$, the requirement for the continued generation $I(1,4,5)P_3$ to sustain long-term Ca^{2+} responses, the rapid depletion of $PI(4,5)P_2$ by PLC in other systems, and the ability of two downstream targets of Vav, Rho and Rac, to interact with PIP5K suggested that an important function of the CD19–Vav complex may be to induce the synthesis of $PI(4,5)P_2$. To determine whether the cross-linking of CD19 to mIg costimulates PIP5K, splenic B lymphocytes were activated by coligating a suboptimal number of mIg with increasing amounts of CD19, and, at the same time, permeabilizing the cells with streptolysin O (SLO) to permit the introduction of $[\gamma^{32}P]ATP$. Lipids were extracted and separated, and the incorporation of $[^{32}P]PO_4$ into PIP_2 determined. mIg alone induced a modest increment in PIP_2 synthesis. Coligating CD19 to mIg increased the synthesis of PIP_2 in a synergistic and dose-related manner (Figure 4A). Cross-linking CD19 alone also caused dose-dependent synthesis of PIP_2, which was lesser in magnitude (Figure 4A).

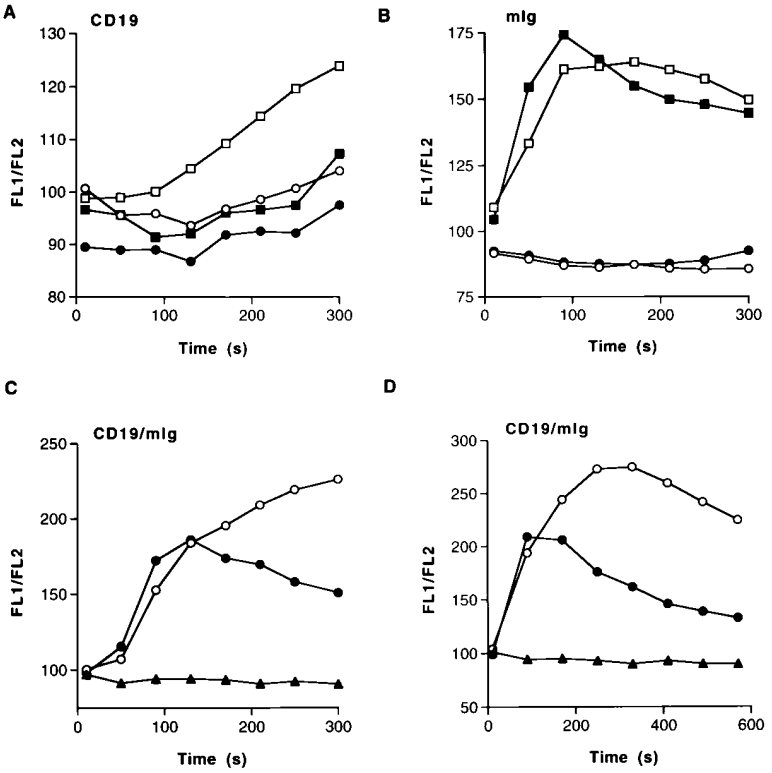

Figure 3. Changes in $[Ca^{2+}]_i$ in B Cells from *Vav*$^{+/+}$ and *Vav*$^{-/-}$ Mice Stimulated by CD19 or mIg Alone or by Cross-linking CD19 to Suboptimal mIg

Splenocytes from *Vav*$^{+/+}$ mice (open symbols) and *Vav*$^{-/-}$ mice (closed symbols) were stained with phycoerythrin-conjugated antibody to CD43, loaded with indo-1, and preincubated with (A) biotinylated F(ab′)$_2$ antibody to CD19 at 10 μg/ml (squares) and 1 μg/ml (circles); (B) biotinylated Fab antibody to κ at 10 μg/ml (squares) and 0.1 μg/ml (circles); (C and D) biotinylated Fab antibody to κ at 0.1 μg/ml in the presence of biotinylated F(ab′)$_2$ antibody to CD19 at 1 μg/ml (circles), or biotinylated Fab isotype control antibody at 0.1 μg/ml together with biotinylated F(ab′)$_2$ isotype control antibody at 1 μg/ml (closed triangles). After 20 sec, avidin was added, and the analysis was continued for (A–C) 5 min or (D) 10 min, gating on CD43$^-$ cells. Changes in $[Ca^{2+}]_i$ are indicated by changes in the ratio of the fluorescence at 400–410 nm (FL1) and at 460–480 nm (FL2). Data are representative of three independent experiments.

To confirm that the PIP_2 induced by CD19 was PI(4,5)P_2, the PIP_2 was deacylated and analyzed by anion-exchange high-performance liquid chromatography. Approximately 90% of the counts were in the GroPI(4,5)P_2 peak, the deacylated product that is derived from PI(4,5)P_2. The deacylated product of PI(3,4)P_2, GroPI(3,4)P_2, was not present (data not shown).

We determined whether Vav participated in this stimulation of PI(4,5)P_2 synthesis by activating splenic B lymphocytes from *Vav*$^{+/+}$ and *Vav*$^{-/-}$ mice. In wild-type cells, ligating large numbers of mIg or CD19 induced the synthesis of PI(4,5)P_2, as did the synergistic interaction of suboptimal numbers of mIg and CD19 (Figure 4B). The synergistic- and mIg-mediated reactions were reduced by approximately 50% in the *Vav*$^{-/-}$ B lymphocytes, and CD19 alone was inactive in these cells (Figure 4B). A stringent requirement of CD19 for Vav was confirmed when the dose-dependent increase in PI(4,5)P_2 induced by CD19 in wild-type B lymphocytes was found to be absent in *Vav*$^{-/-}$ cells (Figure 4C).

Although Rho and Rac have been shown to interact with PIP5K, a recent study has identified a PI(5)P4K that phosphorylates PI5P to generate PI(4,5)P_2 (Rameh et al., 1997). To confirm that CD19 activates a PI(4)P5K rather than a PI(5)P4K, the [^{32}P]PI(4,5)P_2 induced by CD19 was treated with the phosphatase synaptojanin, which preferentially dephosphorylates position 5 of the inositol ring of PI(4,5)P_2 (Woscholski et al., 1995). [^{3}H]PI(4,5)P_2 was added to the reaction as an independent measure of PI(4,5)P_2 hydrolysis and recovery of PIP, since the radiolabel will not be affected by the dephosphorylation. When the [^{32}P]PI(4,5)P_2 induced by CD19 was dephosphorylated by synaptojanin, only 17% of the counts lost from PI(4,5)P_2 were recovered as [^{32}P]PI(4)P, whereas 82% of the hydrolyzed [^{3}H]PI(4,5)P_2 was recovered as [^{3}H]PI(4)P. In two additional experiments, the recoveries of CD19-induced [^{32}P]PI(4,5)P_2 as [^{32}P]PI(4)P following treatment with the 5-phosphatase were 28% and 29%, while the corresponding recoveries for [^{3}H]PI(4,5)P_2 were 94% and 88%. The capacity of the synaptojanin (5)Ptase to cause a preferential loss of label from the [^{32}P]PI(4,5)P_2 induced by CD19 indicates that this phospholipid had been phosphorylated at position 5 through the activation of PIP5K. The residual ^{32}P in the PI(4)P may indicate either that a portion of the substrate of the PIP5K activated by CD19 had already been endogenously labeled by a constitutively active PI4K (Figures 4C, 5A, and 6A), or that CD19 also activates a PI(5)P4K.

CD19 resides in a complex with CD21 and CD81, and the latter has been shown to amplify the Ca^{2+} response when coligated with mIg (Matsumoto et al., 1993). The association of CD81 with CD19 requires the extracellular domain of CD19 (Bradbury et al., 1993; Matsumoto et al., 1993). We determined whether the effects of CD19 on the activation of PIP5K and maintenance of elevated $[Ca^{2+}]_i$ required CD81 by examining these reactions in the Daudi B cell transfectants expressing the CD4–CD19 chimeras. The transfectants were activated by coligating a suboptimal number of mIg with incremental numbers of ΔEC and Y391F, respectively, to which anti-CD4 had been bound. Synthesis of PI(4,5)P_2 was measured by introducing [γ^{32}P]ATP into the SLO-permeabilized cells and determining the incorporation of [^{32}P]PO_4 into PI(4,5)P_2. ΔEC caused a dose-related synergistic activation of PIP5K when cross-linked to mIg (Figure 5A); it did not augment the synthesis of PI(4,5)P_2 when ligated

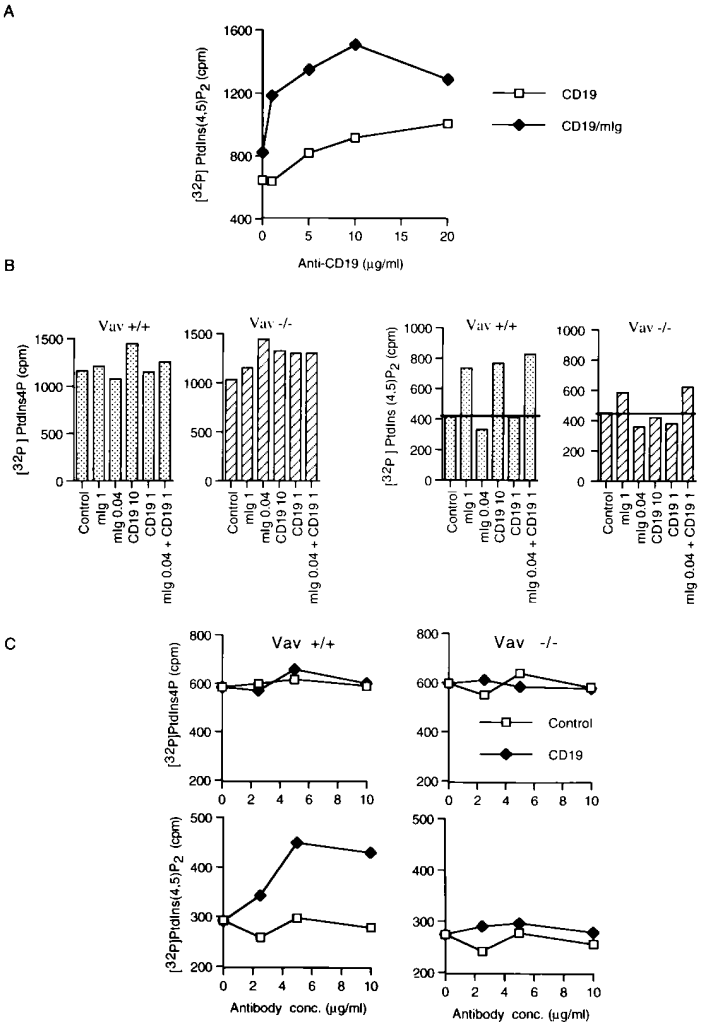

Figure 4. Synthesis of $[^{32}P]PI(4,5)P_2$ in B Cells from *Vav*$^{+/+}$ and *Vav*$^{-/-}$ Mice

(A) Splenic B cells were preincubated with incremental concentrations of biotinylated Fab antibody to CD19 in the absence or presence of a suboptimal concentration of biotinylated Fab antibody to κ (0.04 μg/ml). In this experiment and those depicted in (B) and (C), the cell-bound antibodies were cross-linked by avidin for 1 min in buffer containing SLO and $[\gamma^{32}P]ATP$, after which the synthesis of $[^{32}P]PI4P$ (in B and C) and $[^{32}P]PI(4,5)P_2$ was measured.

(B) B cells from *Vav*$^{+/+}$ mice (92% B220$^+$) and *Vav*$^{-/-}$ mice (91% B220$^+$) were preincubated with the following biotinylated antibody fragments: control Fab (10 μg/ml); Fab anti-κ (1 μg/ml and 0.04 μg/ml); Fab anti-CD19 (10 μg/ml and 1 μg/ml); and Fab anti-κ (0.04 μg/ml) in the presence Fab anti-CD19 (1 μg/ml).

(C) B cells from *Vav*$^{+/+}$ mice (89% B220$^+$) and *Vav*$^{-/-}$ mice (85% B220$^+$) were preincubated with incremental concentrations of biotinylated Fab monoclonal antibody to CD19 or biotinylated control Fab antibody. Data are representative of three independent experiments.

alone. Endogenous CD19 alone also does not activate PIP5K in these cells (data not shown). Y391F was inactive in the synergistic response with mIg, even though it was expressed at 5-fold higher numbers per cell than the ΔEC receptor. Coligating ΔEC or Y391F to mIg did not induce synthesis of PI4P.

The two chimeric receptors were also assessed for their ability to costimulate increases in $[Ca^{2+}]_i$. By adjusting the concentrations of anti-CD4, equivalent numbers of ΔEC and Y391F were ligated alone, or a suboptimal number of mIg were ligated alone with anti-Ig, or mIg and CD4-CD19 were cross-linked together on transfectants that had been loaded with indo-1. A synergistic increase in $[Ca^{2+}]_i$ occurred when ΔEC was cross-linked to mIg, but Y391F lacked this function (Figure 5B). Similar findings were obtained with additional clones of these transfectants. Therefore, CD81 is not required for either the activation by CD19 of PIP5K or a sustained increase in $[Ca^{2+}]_i$, and the Vav dependence of these reactions is confirmed. However, CD81 may have contributed to the initial synergistic increase in $[Ca^{2+}]_i$ induced by intact CD19 in Vav-deficient B cells (Figures 3C and 3D). The Y391F chimera, which does not associate with CD81, lacked this response in the Daudi B cells (Figure 5B).

We wished to determine whether a guanine nucleotide–binding protein mediated the activation of PIP5K by CD19 because of the involvement of the GEF, Vav, in this reaction. The transformed murine B lymphoma line, Bal17, was stimulated by cross-linking CD19 and permeabilized with SLO in the presence of $[\gamma^{32}P]ATP$ and increasing concentrations of GDPβS. Measurement of the synthesis of $PI(4,5)P_2$ demonstrated that GDPβS inhibited the activation of PIP5K in a dose-related manner (Figure 6A). To assess whether Rho was the GDPβS-inhibitable GTPase, we introduced into Bal17 cells the *Clostridium botulinum* C3 exoenzyme, which specifically ADP ribosylates and inactivates Rho (Aktories and Hall, 1989). Greater than 95% ADP ribosylation of Rho (Figure 6B) had no effect on the capacity of CD19 or on that of the positive control, GTPγS, to induce the synthesis of $PI(4,5)P_2$ (Figure 6C). These observations are consistent with a GTP-dependent, but Rho-independent, activation of PIP5K by CD19 and Vav, and indicate that another GTPase may be relevant, such as Rac,

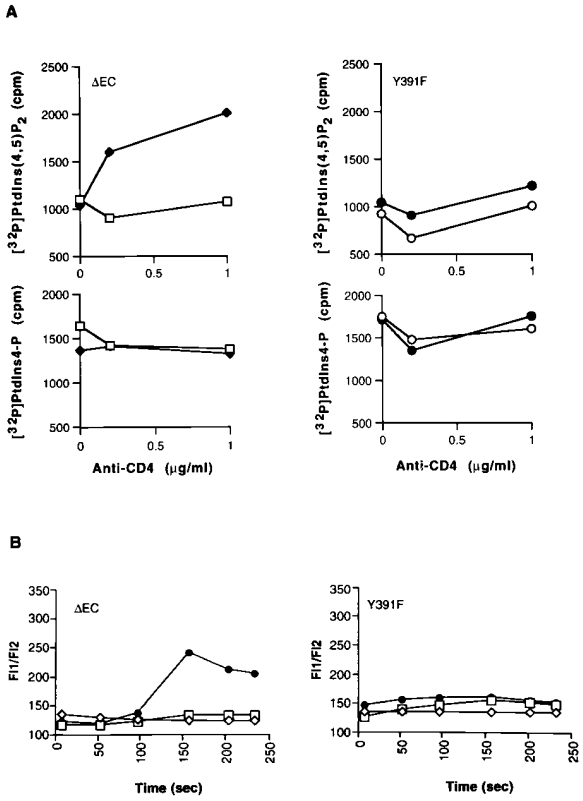

Figure 5. Synthesis of [^{32}P]PI(4,5)P_2 and Changes in [Ca^{2+}]$_i$ in Daudi B Lymphoblastoid Cells Costimulated by mIg and the CD4/CD19 Chimeras, ΔEC, and Y391F

(A) The transfectants were preincubated with incremental concentrations of the Fab fragment of mouse monoclonal anti-CD4 in the absence (open symbols) or presence (closed symbols) of a suboptimal concentration of Fab mouse monoclonal anti-human IgM (0.01 μg/ml). Because of higher expression on the transfectants of Y391F than of ΔEC, the former bound 5-fold more anti-CD4 than did the latter, as determined by flow cytometry. The cell-bound antibodies were cross-linked by addition of F(ab′)$_2$ goat antibody to mouse IgG. After 1 min, buffer containing SLO and [γ^{32}P]ATP was added and the incubation was continued for 1 min, after which the synthesis of [^{32}P]PI4P and [^{32}P]PI(4,5)P_2 was determined.

(B) Daudi transfectants were loaded with indo-1 and preincubated with concentrations of biotinylated Fab anti-CD4 that yielded equivalent binding to the transfectants (open diamonds), a single concentration of biotinylated Fab anti-IgM that was below the threshold for raising [Ca^{2+}]$_i$ (open squares), or both (closed circles). The cells were washed; avidin was added to cross-link the cell-bound antibodies; and indo-1 fluorescence was measured. Shown is the ratio of the fluorescence at 400–410 nm (FL1) and at 460–480 nm (FL2). Data are representative of three independent experiments.

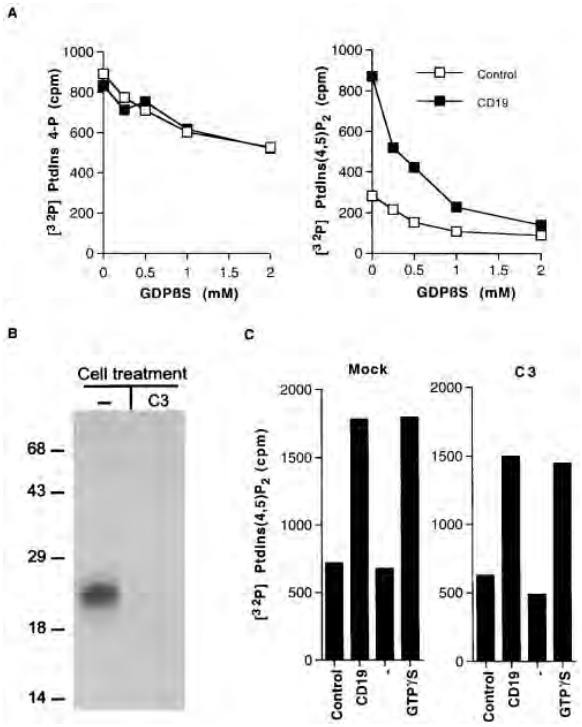

Figure 6. Effects of GDPβS and *C. botulinum* C3 Transferase on Synthesis of [^{32}P]PI(4,5)P_2 in B Cells Stimulated by CD19

(A) Bal17 cells were preincubated with 5 μg/ml of the biotinylated Fab fragments of antibody to CD19 or the nonspecific control antibody. The cell-bound antibodies were cross-linked for 1 min by addition of avidin (20 μg/ml) in buffer containing SLO and [γ^{32}P]ATP alone or with the indicated concentrations of GDPβS, after which the synthesis of [^{32}P]PI4P and [^{32}P]PI(4,5)P_2 was measured.

(B) Bal17 cells were electroporated in the absence (-) or presence (C3) of 100 μg/ml C3 transferase and subsequently cultured for 5 hr. An aliquot of the cells was washed, lysed, and incubated with C3 transferase and ^{32}P-NAD. The proteins in the lysate were separated by SDS-PAGE and subjected to autoradiography to determine the extent of in vivo ADP ribosylation of Rho.

(C) The remaining mock or C3 transferase–treated cells were preincubated with 5 μg/ml of the biotinylated Fab fragments of antibody to CD19 or with control antibody. The cell-bound antibodies were cross-linked for 1 min by addition of avidin (20 μg/ml) in buffer containing SLO and [γ^{32}P]ATP. For stimulation with GTPγS, buffer containing SLO and [γ^{32}P]ATP alone or with 100 μM GTPγS was added to cells. After 1 min, the reactions were stopped and the synthesis of [^{32}P]PI(4,5)P_2 was measured. Data are representative of three independent experiments.

which has been found to activate PIP5K in another hematopoietic cell type, the platelet (Hartwig et al., 1995).

Costimulation of JNK by mIg and CD19 Requires Vav

The finding that CD19 recruits the function of Vav, coupled with the known ability of Vav to activate JNK through Rac and Cdc42 (Crespo et al., 1996), offered a possible mechanism for the costimulation by CD19 of this MAP kinase. B lymphocytes from *Vav*$^{+/+}$ and *Vav*$^{-/-}$ mice were stimulated by cross-linking cell-bound Fab fragments of antibodies to κ and CD19 alone or together, followed by immunoprecipitation of JNK and, for comparison, ERK2, from cell lysates. Using in vitro kinase assays, we measured the activities of JNK by phosphorylation of a GST-c-Jun1–194 fusion protein, and of ERK2 by phosphorylation of GST-Elk1C fusion protein. Ligating mIg or CD19 alone did not substantially activate either MAP kinase (Figure 7A) in either type of B lymphocyte; in other experiments, higher amounts of ligated mIg induced modest activation of ERK2 (data not shown). Coligating mIg and CD19 on wild-type B lymphocytes caused a synergistic activation of both JNK and ERK2. In the absence of Vav, costimulation of ERK2 was maintained, but activation of JNK was diminished by up to

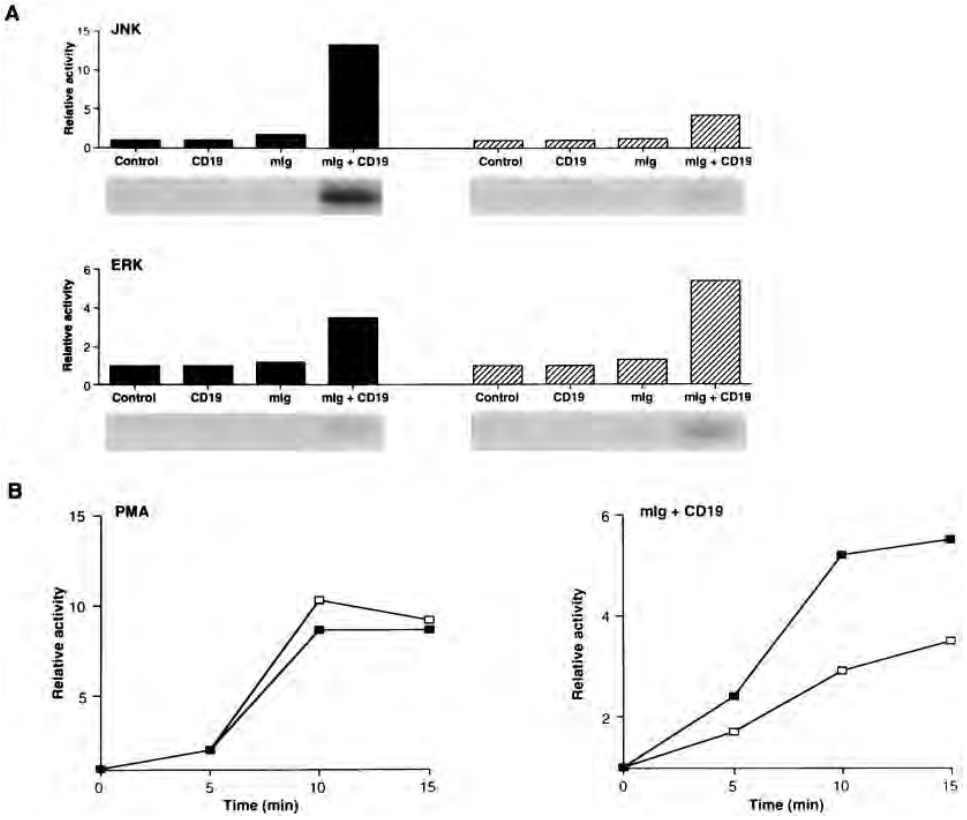

Figure 7. Activation of JNK and ERK by Coligated CD19 and mIg in B Cells from *Vav*$^{+/+}$ and *Vav*$^{-/-}$ Mice

(A) B cells from *Vav*$^{+/+}$ mice (solid bars) and *Vav*$^{-/-}$ mice (hatched bars) were incubated with biotinylated Fab fragments of isotype-matched, nonspecific control antibody (10 μg/ml), or with Fab fragments of monoclonal antibody to CD19 (5 μg/ml) and κ (5 μg/ml) alone or together. Cells were washed and stimulated for 10 min at 37°C by addition of avidin (20 μg/ml). Stimulation was stopped by addition of lysis buffer, and replicate samples of the lysates were subjected to immunoprecipitation with antibodies to ERK2 or JNK1. The immunoprecipitates were assayed for ERK and JNK activities by phosphorylation, in the presence of [γ^{32}P]ATP, of the fusion proteins GST-Elk1C and GST-c-Jun1–194, respectively (Tooze et al., 1997). Shown are the autoradiographs of the GST fusion proteins and their relative incorporation of ^{32}P.

(B) (Left) B cells from *Vav*$^{+/+}$ mice (closed squares) and *Vav*$^{-/-}$ mice (open squares) were incubated with buffer alone or containing 500 ng/ml PMA for timed intervals, after which cells were lysed. The activity of JNK in the lysates was assayed and expressed relative to that of cells treated with buffer only. (Right) B cells from *Vav*$^{+/+}$ mice (closed squares) and *Vav*$^{-/-}$ mice (open squares) were incubated with biotinylated Fab fragments of antibodies to CD19 and κ together at doses (0.5 μg/ml) that alone were nonstimulatory, or with Fab fragments of an isotype-matched, nonspecific control antibody (1 μg/ml). The cells were washed and stimulated by addition of avidin (20 μg/ml) and incubation continued for timed intervals, after which the cells were lysed. The activity of JNK in the lysates was assayed and expressed relative to that of cells treated with control antibody. Data are representative of three independent experiments.

80% (Figure 7A). Analysis of the time course of JNK activation by mIg/CD19 coligation demonstrated that over the entire 15 min period of observation, the costimulation of JNK was diminished in B lymphocytes from *Vav*$^{-/-}$ mice, whereas that by phorbol myristate acetate (PMA) was independent of Vav (Figure 7B). Hence, the activation of JNK by mIg and CD19 is mediated, in part, by Vav, but activation of ERK2, which may be mediated by another GTPase, Ras, is not. The residual activation of JNK in *Vav*$^{-/-}$ B lymphocytes may be caused by Ras-dependent activation of Rac (Coso et al., 1995; Minden et al., 1995).

Discussion

CD19 serves as a membrane-anchored adaptor protein that enhances activation of the B lymphocyte by mIg. When tyrosine phosphorylated, it recruits cytoplasmic effector proteins containing SH2 domains that amplify signaling by the mIg complex, the first example of which was the binding by phosphorylated tyrosines-482 and -513 of PI3K (Tuveson et al., 1993), which has been shown to contribute to mIg-induced increase in $[Ca^{2+}]_i$ (Buhl et al., 1997). This general concept is extended in the present study by finding that tyrosine-391 of CD19 binds Vav to activate PIP5K and elevate $[Ca^{2+}]_i$ and to costimulate JNK. Thus, the phosphotyrosine-based adaptor function of CD19 augments the stimulation by mIg of at least two lipid kinases and a protein kinase.

The role of CD19 as a costimulator of mIg-induced activation of the B lymphocyte requires its cross-linking to mIg (Carter and Fearon, 1992). Because of the association of CD19 with CD21, this process occurs physiologically when antigen has been tagged with C3d. There

are two possible explanations for this requirement: juxtaposition of CD19, with its associated cytosolic proteins, to mIg creates a more effective signaling complex, and the tyrosine phosphorylation of CD19, which mediates the binding of these cytosolic proteins, is regulated by mIg. Although CD19 can be phosphorylated when either it or mIg is ligated alone, the present work shows that cross-linking CD19 to mIg causes a 10- to 20-fold greater tyrosine phosphorylation of CD19 than when either receptor was ligated alone (Figure 1). This is the most proximal synergistic reaction of CD19 and mIg that has been observed. This synergistic phosphorylation of CD19 is probably relevant to signaling since it was accompanied by a comparable increase in the binding of Vav (Figure 1) and PI3K (data not shown). The mechanism of this effect may involve the phosphorylation of CD19 by protein kinases associated with the mIg complex, such as Lyn or Syk; by other kinases that are activated by mIg, such as Btk; or by the more effective activation of the Lyn or Fyn that is associated with CD19.

In any event, this finding indicates that synergistic signaling by coligated CD19 and mIg occurs at an early first step, and emphasizes that an essential characteristic of stimulatory antigen must be its physical association with a ligand for the CD19–CD21 complex, either through attachment of C3d or possibly by its presence on membranes bearing a ligand for this complex, such as CD23. An earlier finding that coligating CD19 to mIgM on Daudi B lymphoblastoid cells did not increase the tyrosine phosphorylation of CD19 (Li et al., 1997) may reflect the more robust activation of kinases by mIgM in this cell having a deficiency of the tyrosine phosphatase SHP-1 (Delibrias et al., 1997).

The first signal-transducing function that was described for CD19 was the elevation of $[Ca^{2+}]_i$ (Pezzutto et al., 1987). This response, like tyrosine phosphorylation, can occur when CD19 or mIg is ligated alone, but is most pronounced when CD19 and mIg are cross-linked together (Carter et al., 1991). We established a causal relationship between tyrosine phosphorylation and the Ca^{2+} response by finding that the enhanced phosphorylation of CD19 was accompanied by increased association with Vav (Figure 1); that phosphorylated tyrosine-391 bound Vav (Figure 2); and that the absence of Vav (Figure 3), or mutation of tyrosine-391 (Figure 5), impaired the CD19-dependent Ca^{2+} response. These studies have also provided a reasonable explanation for the contribution of Vav to the Ca^{2+} response mediated by CD19, which is the activation of PIP5K leading to the synthesis of $PI(4,5)P_2$ (Figures 4–6). The rapid depletion of $PI(4,5)P_2$ by PLC, which in other cellular systems occurs within seconds of receptor-mediated stimulation (Stephens et al., 1993), would impair the continued generation of $I(1,4,5)P_3$ unless stimulation was also coupled to the activation of a biosynthetic pathway for $PI(4,5)P_2$. mIg is coupled to the activation of PIP5K, but only when high concentrations of ligand are used (Figure 4B). The costimulatory effect on the generation of $I(1,4,5)P_3$ occurring when CD19 is cross-linked to suboptimal amounts of mIg would therefore require another means by which the synthesis of $PI(4,5)P_2$ could be increased above basal levels. The interaction of CD19 with Vav meets this requirement, contributing to the long-term Ca^{2+} response in B lymphocytes that have been costimulated by mIg and CD19 (Figures 3C and 3D). These findings may explain early studies that found that GTPγS enhanced, and GDPβS suppressed, mIg-induced generation of $I(1,4,5)P_3$ (Gold et al., 1987; Harnett and Klaus, 1988).

We have not determined whether the increased availability of $PI(4,5)P_2$ accounts entirely for the effect of CD19 on $[Ca^{2+}]_i$. For example, even in the absence of Vav, coligating CD19 to mIg caused an initial, synergistic increase in $[Ca^{2+}]_i$ (Figure 3) and diminished, but residual, synthesis of $PI(4,5)P_2$, which may reflect compensation by Vav2 in the *Vav*$^{-/-}$ cells (Schuebel et al., 1996). However, all activities were lost with Y391F, the chimeric CD4–CD19 fusion protein lacking the extracellular domain of CD19 and the site for interaction with Vav (Figure 5). Since this domain mediates the interaction of CD19 with CD81, and CD81 alone has been shown also to enhance synergistically the increase in $[Ca^{2+}]_i$ induced by mIg (Matsumoto et al., 1993), the early increment in $[Ca^{2+}]_i$ may be mediated by CD81. The recruitment of this function of CD81 by CD19 would represent an extracellular, rather than intracellular, "adaptor" function for the receptor. However, even the absence of any synergistic increase in $[Ca^{2+}]_i$ with the Y391F mutant cannot be taken as proof of a role only for Vav or Vav2 because other cellular proteins may interact with this tyrosine, as has been suggested by the requirement of tyrosine-391 for ERK2 costimulation (Li et al., 1997), a response that does not require Vav (Figure 6).

Vav has not been described previously as activating PIP5K, although focal regulation of the level of $PI(4,5)P_2$, which interacts with actin-binding proteins (Janmey, 1994; Hartwig et al., 1995), could contribute to several of its effects on the organization of the cytoskeleton (Khosravi-Far et al., 1994). Two GTPase targets of Vav, Rho and Rac, interact with PIP5K. Although we obtained evidence for the involvement of a guanine nucleotide–binding protein by inhibiting CD19-mediated activation of PIP5K with GDPβS (Figure 5), we did not identify the GTPase mediating PIP5K activation because ADP ribosylation of Rho did not impair this reaction (Figure 5). These findings suggest, by exclusion of Rho, an involvement of Rac, but this pathway leading from Vav to PIP5K remains to be defined.

CD19 has been found recently to costimulate ERK2, JNK, and p38 (Tooze et al., 1997), and one report has shown a requirement for tyrosine-391 in the activation of ERK2 (Li et al., 1997). Although Vav had been described as a GEF for Ras, which would have been consistent with tyrosine-391 mediating the costimulation of ERK2 by this pathway, subsequent studies have indicated a role for Vav in the activation of the Rho family of GTPases rather than Ras (Bustelo et al., 1994). Consistent with these more recent findings, we found that Vav contributed to activation of JNK but not ERK2 (Figure 6). Therefore, tyrosine-391, whether phosphorylated or not, may interact with another cytosolic protein in addition to Vav, to mediate this Ras-dependent MAP kinase pathway.

The CD19–CD21 complex links innate immune recognition of antigen to the acquired immune response, enabling the B lymphocyte to bias its response to antigens

of microbial origin that have activated the complement system. Both receptors are required for the normal development of the germinal center in which occur the essential B lymphocyte responses of isotype switching, somatic mutation of mIg, selection, and the generation of memory B lymphocytes. The present finding that CD19 recruits the product of a protooncogene, *Vav*, to regulate lipid and protein kinases that serve two distinct signaling pathways is consistent with the importance of these biological functions of the CD19-CD21 complex.

Experimental Procedures

Reagents

The following reagents were purchased: Phosphatidylserine, PI4P, PI(4,5)P_2, GTPγS, GDPβS, avidin, and antibody to Thy1.2 (Sigma), silicia gel-60 thin layer chromatography plates (Whatman), SLO (Murex Biotech), indo-1-AM (Molecular Probes), biotinylated CD19 peptides (Quality Controlled Biochemicals), streptavidin agarose and protein A–trisacyl (Pierce), glutathione sepharose and GammaBind Plus Sepharose (Pharmacia Biotech), [γ^{32}P]ATP, and [^{32}P]NAD (Amersham). The construct for *C. botulinum* C3 exoenzyme GST fusion protein was a gift from Alan Hall and the constructs for GST-c-Jun1–194 and GST-Elk1C fusion proteins were provided by Doreen Cantrell and Richard Treisman, respectively. Active C3 transferase was purified by removal of GST by thrombin cleavage. Recombinant synaptojanin was kindly supplied by R. Woscholski.

Antibodies

The following antibodies were used: 1D3 rat IgG2a antibody to mouse CD19 (Krop et al., 1996), DA4.4 mouse anti-human IgM (Carter et al., 1991), rabbit antibodies to the cytoplasmic domains of human CD19 (Tuveson et al., 1993) and mouse CD19 (Krop et al., 1996), LO-MK-1 rat IgG2a antibody to mouse κ and IR 418 rat IgG2a myeloma (Zymed), F(ab′)$_2$ goat antibodies to human IgM (Tago) and mouse IgG (Jackson), monoclonal antibody to Vav, rabbit polyclonal antibody to Vav, 4G10 anti-phophosotyrosine antibody (Upstate Biotechnology), monoclonal antibody to CD4 (Caltag), G151–333.8 mouse monoclonal antibody to mouse JNK1, and phycoerythrin-conjugated S7 rat monoclonal antibody to mouse CD43 (Pharmingen). Fab fragments were produced by papain digestion and were biotinylated with ImmunoPure Sulfo-NHS-Biotin (Pierce). Serum 122 rabbit antiserum to ERK2 was provided by Christopher J. Marshall.

Cells

Daudi cells expressing the ΔEC and Y391F CD4-CD19 chimeras were generated as described (Matsumoto et al., 1993; Li et al., 1997). Bal17 murine B lymphoma cells were maintained in RPMI plus 5% fetal calf serum and 50 μM 2-mercaptoethanol. Splenic B cells were enriched by depletion of T cells with anti-Thy1.2 (Sigma) and rabbit complement (Harlan Sera Lab) followed by centrifugation over Lympholyte-M (Cedar Lane).

Immunoprecipitation

Biotinylated peptides (5 μM) were incubated with 0.2 ml of a 25% slurry of streptavidin-agarose in phosphate-buffered saline for 1 hr at 4°C followed by washing. The beads were incubated with Nonidet P-40 (NP-40) lysates (Tuveson et al., 1993) of 2.5×10^7 Daudi cells for 30 min at 20°C, and the bound proteins were eluted, resolved by SDS-PAGE, transferred to nitrocellulose, and immunoblotted with antibody to Vav followed by enhanced chemiluminescence. Chimeric CD4/CD19 receptors were immunoprecipitated from cell lysates by incubation with antibody to CD4 followed by protein A–sepharose.

After stimulation, 1×10^8 splenic B cells were lysed in buffer containing 1% NP-40, 0.1% SDS, 50 mM Tris (pH 7.4), 150 mM NaCl, 0.5 mM EDTA, 20 mM tetrasodium pyrophosphate, 10 mM sodium flouride, 1 mM sodium orthovanadate, 10 mM sodium molybdate, 10 mM iodoacetamide, 10 μM leupeptin, antipain (2 μg/ml), 1 μM pepstatin A, chymostatin (6 μg/ml), aprotinin (1 μg/ml), and 4-(2-aminoethyl)-benzenesuflonyl fluoride (1 μg/ml) (Calbiochem). Lysates were precleared by incubation with a nonspecific rat IgG2a and rabbit anti-rat IgG followed by protein A. CD19 was immunoprecipitated from cell lysates by incubation with 1D3 rat antibody to CD19 and rabbit anti-rat IgG followed by protein A trisacryl.

Biosynthetic Labeling and Quantitation of Phospholipids

Cells in Hanks' balanced salt solution without Mg^{2+}or Ca^{2+} were preincubated with appropriate Fab antibody fragment for 15 min at room temperature, washed, and activated by addition of avidin or F(ab′)$_2$ goat antimouse immunoglobulin at 20 μg/ml in intracellular buffer (Alexander et al., 1989) at 37°C. Cells were permeabilized at 37°C by adding 50 μl of SLO (0.8 IU/ml) containing 10 μCi [^{32}P]γATP, giving a final concentration of 100 μM ATP. In some experiments cells were stimulated and permeabilized at the same time. After 1 min of permeabilization, the reaction was quenched with 600 μl of chloroform/methanol/HCl (1:2:1) containing 10 μg of phosphatidylserine. Two hundred microliters of chloroform and 200 μl of 2.4 M HCl were added and the lower phase was washed with 800 μl of methanol:1 M HCl (1:1). The lipid extract was dried under nitrogen and resuspended in chloroform for spotting on potassium oxalate–impregnated thin-layer chromatography (TLC) plates. The TLC plates were developed in chloroform/methanol/acetone/acetic acid/$H_2$0 (80:30:26:24:14), and the [^{32}P] incorporated into PIP; PIP$_2$ was quantitated using a Packard-Bell InstantImager.

Preparation of PI(4,5)P_2 Substrate and 5-phosphatase Assay

CD19-induced, ^{32}P-labeled PI(4,5)P_2 was recovered from Bal17 cells by lipid extraction and TLC. [^{3}H]PI(4,5)P_2 (0.05 mCi) and sufficient unlabeled PIP$_2$ were added to each to yield 36 μg of PI(4,5)P_2 per extract, dried under nitrogen, and sonicated in 120 μl 0.5% CHAPS, 0.2 M Tris (pH 7.4). Synaptojanin was incubated with 40 μl of [^{3}H]PI(4,5)P_2/[^{32}P]PI(4,5)P_2 in 120 μl containing 5 mM $MgCl_2$, 0.5 mM EGTA, 70 mM Tris (pH 7.4), and 0.17% CHAPS for 2 hr at 37°C. The phospholipids were separated by TLC, the spots corresponding to PIP and PIP$_2$ identified by iodine vapor, scraped, and counted by liquid scintillation.

ADP Ribosylation with C3 Exoenzyme

Replicate 0.8 ml aliquots of Bal17 cells at 2×10^7/ml in phosphate-buffered saline/10 mM glucose/1 mM $MgCl_2$ in the presence or absence of 100 μg/ml C3 exotoxin were subjected to a discharge of 0.4 V from a 25 μF capacitor using the gene pulser (Bio-Rad Laboratories). After 10 min at 4°C, cells were resuspended at 1–2 $\times$ 10^5/ml in culture media and allowed recover for 5 hr at 37°C before stimulation or ADP ribosylation of lysates (Yamamoto et al., 1993).

Acknowledgments

We thank D. Cantrell for help in the permeabilization studies, L. Stephens for the HPLC analysis of PIP$_2$, T. Bridges for assistence with C3 exoenzyme, J. Saklatvala for assistance with MAP kinase assays and R. Woscholski for recombinant synaptojanin. This work was supported by the Wellcome Trust (D. T. F., L. O., R. T.), and the Arthritis Foundation and the Office of Research and Development, Medical Research Service, Department of Veterans Affairs (R. H. C.), and the Medical Research Council (M. T., V. T.).

Received December 9, 1997; revised March 30, 1998.

References

Aktories, K., and Hall, A. (1989). Botulinum ADP-ribosylation transferase: a new tool to study low molecular weight GTP-binding proteins. Trends Pharmacol. Sci. *10*, 415–418.

Alexander, D.R., Hexham, J.M., Lucas, S.C., Graves, J.D., Cantrell, D.A., and Crumpton, M.J. (1989). A protein kinase C pseudosubstrate peptide inhibits phosphorylation of CD3 antigen in streptolysin-O-permeabilized human T cells. Biochem. J. *260*, 893–901.

Billips, L.G., Nunez C. A., Bertrand, F.E., Stankovic, A.K., Gartland,

G.L., Burrows, P.D., and Cooper, M.D. (1995). Immunoglobulin recombinase gene activity is modulated reciprocally by interleukin 7 and CD19 in B cell progenitors. J. Exp. Med. *182*, 973–982.

Bradbury, L.E., Goldmacher, V.S., and Tedder, T.F. (1993). The CD19 signal transduction complex of B lymphocytes: deletion of the CD19 cytoplasmic domain alters signal transduction but not complex formation with TAPA-1 and Leu 13. J. Immunol. *151*, 2915–2927.

Buhl, A.M., Pleiman, C.M., Rickert, R.C., and Cambier, J.C. (1997). Qualitative regulation of B cell antigen receptor signaling by CD19: selective requirement for PI3-kinase activation, inositol-1,4,5-trisphosphate production and Ca^{2+} mobilization. J. Exp. Med. *186*, 1897–1910.

Bustelo, X.R., and Barbacid, M. (1992). Tyrosine phosphorylation of the vav proto-oncogene product in activated B cells. Science *256*, 1196–1199.

Bustelo, X.R., Ledbetter, J.A., and Barbacid, M. (1992). Product of vav proto-oncogene defines a new class of tyrosine protein kinase substrates. Nature *356*, 68–71.

Bustelo, X.R., Suen, K.L., Leftheris, K., Meyers, C.A., and Barbacid, M. (1994). Vav cooperates with Ras to transform rodent fibroblasts but is not a ras GDP/GTP exchange factor. Oncogene *9*, 2405–2413.

Carter, R.H., and Fearon, D.T. (1992). CD19: lowering the threshold for antigen receptor stimulation of B lymphocytes. Science *256*, 105–107.

Carter, R.H., Tuveson, D.A., Park, D.J., Rhee, S.G., and Fearon, D.T. (1991). The CD19 complex of B lymphocytes: activation of phospholipase C by a protein tyrosine kinase-dependent pathway that can be enhanced by the membrane IgM complex. J. Immunol. *147*, 3663–3671.

Chong, L.D., Traynor-Kaplan, A., Bokoch, G.M., and Schwartz, M.A. (1994). The small GTP-binding protein Rho regulates a phosphatidylinositol 4-phosphate 5-kinase in mammalian cells. Cell *79*, 507–513.

Coso, O.A., Chiariello, M., Yu, J.C., Teramoto, H., Crespo, P., Xu, N., Miki, T., and Gutkind, J.S. (1995). The small GTP-binding proteins Rac1 and Cdc42 regulate the activity of the JNK/SAPK signaling pathway. Cell *81*, 1137–1146.

Crespo, P., Bustelo, X.R., Aaronson, D.S., Coso, O.A., Lopez-Barahona, M., Barbacid, M., and Gutkind, J.S. (1996). Rac-1 dependent stimulation of the JNK/SAPK signaling pathway by Vav. Oncogene *13*, 455–460.

Crespo, P., Schuebel, K.E., Ostrom, A.A., Gutkind, J.S., and Bustelo, X.R. (1997). Phosphotyrosine-dependent activation of Rac-1 GDP/GTP exchange by the vav proto-oncogene product. Nature *385*, 169–172.

Delibrias, C.C., Floettmann, J.E., Rowe, M., and Fearon, D.T. (1997). Downregulated expression of SHP-1 in Burkitt lymphomas and germinal center B lymphocytes. J. Exp. Med. *186*, 1575–1583.

Dempsey, P.W., Allison, M.E., Akkaraju, S., Goodnow, C.C., and Fearon, D.T. (1996). C3d of complement as a molecular adjuvant: bridging innate and acquired immunity. Science *271*, 348–350.

Engel, P., Zhou, L.J., Ord, D.C., Sato, S., Koller, B., and Tedder, T.F. (1995). Abnormal B lymphocyte development, activation, and differentiation in mice that lack or overexpress the CD19 signal transduction molecule. Immunity *3*, 39–50.

Gold, M.R., Jakway, J.P., and DeFranco, A.L. (1987). Involvement of a guanine-nucleotide-binding component in membrane IgM-stimulated phosphoinositide breakdown. J. Immunol. *139*, 3604–3613.

Han, J., Balaka, D., Wei, W., van Aelst, L., Mosteller, R.D., Khosravi-Far, R., Westwick, J.K., Der, C.J., and Broek, D. (1997). Lck regulates Vav activation of members of the Rho family of GTPases. Mol. Cell Biol. *17*, 1346–1353.

Han, J., Luby-Phelps, K., Das, B., Shu, X., Xia, Y., Mosteller, R.D., Krishna, M., Falck, J.R., White, M.A., and Broek, D. (1998). Role of the substrates and products of PI3-kinase in the regulating activation of the rac-related guanosine triphosphateses by Vav. Science *279*, 558–560.

Harnett, M.M., and Klaus, G.G. (1988). G protein coupling of antigen receptor-stimulated polyphosphoinositide hydrolysis in B cells. J. Immunol. *140,* 3135–3139.

Hartwig, J.H., Bokoch, G.M., Carpenter, C.L., Janmey, P.A., Taylor, L.A., Toker, A., and Stossel, T.P. (1995). Thrombin receptor ligation and activated Rac uncap actin filament barbed ends through phosphoinositide synthesis in permeabilized human platelets. Cell *82*, 643–653.

Janmey, P.A. (1994). Phosphoinositides and calcium as regulators of cellular actin assembly and disassembly. Annu. Rev. Physiol. *56*, 169–191.

Katzav, S., Martin-Zanca, D., and Barbacid, M. (1989). vav, a novel human oncogene derived from a locus ubiquitously expressed in hematopoietic cells. EMBO J. *8*, 2283–2290.

Khosravi-Far, R., Chrzanowska-Wodnicka, M., Solski, P.A., Eva, A., Burridge, K., and Der, C.J. (1994). Dbl and Vav mediate transformation via mitogen-activated protein kinase pathways that are distinct from those activated by oncogenic Ras. Mol. Cell. Biol. *14*, 6848–6857.

Krop, I., de Fougerolles, A.R., Hardy, R.R., Allison, M., Schlissel, M.S., and Fearon, D.T. (1996). Self-renewal of B-1 lymphocytes is dependent on CD19. Eur. J. Immunol. *26*, 238–242.

Li, X., Sandoval, D., Freeberg, L., and Carter, R.H. (1997). Role of CD19 tyrosine 391 in the synergistic activation of B lymphocytes by coligating of CD19 and membrane Ig. J. Immunol. *158*, 5649–5657.

Margolis, B., Hu, P., Katzav, S., Li, W., Oliver, J.M., Ullrich, A., Weiss, A., and Schlessinger, J. (1992). Tyrosine phosphorylation of vav proto-oncogene product containing SH2 domain and transcription factor motifs. Nature *356*, 71–74.

Matsumoto, A.K., Martin, D.R., Carter, R.H., Klickstein, L.B., Ahearn, J.M., and Fearon, D.T. (1993). Functional dissection of the CD21/CD19/TAPA-1/Leu-13 complex of B lymphocytes. J. Exp. Med. *178*, 1407–1417.

Minden, A., Lin, A., Claret, F.X., Abo, A., and Karin, M. (1995). Selective activation of the JNK signaling cascade and c-Jun transcriptional activity by the small GTPases Rac and Cdc42Hs. Cell *81*, 1147–1157.

Pezzutto, A., Dorken, B., Rabinovitch, P.S., Ledbetter, J.A., Moldenhauer, G., and Clark, E.A. (1987). CD19 monoclonal antibody HD37 inhibits anti-immunoglobulin-induced B cell activation and proliferation. J. Immunol. *138*, 2793–2799.

Raab, M., da Silva, A.J., Findell, P.R., and Rudd, C.E. (1997). Regulation of Vav-SLP-76 binding by ZAP-70 and its revelance to TCRz/CD3 induction of interleukin-2. Immunity *6*, 155–164.

Rameh, L.E., Tolias, K.F., Duckworth, B.C., and Cantley, L.C. (1997). A new pathway for the synthesis of phosphatidylinositol-4,5-bisphosphate. Nature *390*, 192–196.

Reif, K., Buday, L., Downward, J., and Cantrell, D.A. (1994). SH3 domains of the adaptor molecule Grb2 complex with two proteins in T cells: the guanine nucleotide exchange protein Sos and a 75-kDa protein that is a substrate for the T cell antigen receptor-activated tyrosine kinases. J. Biol. Chem. *269*, 14081–14087.

Ren, X.-D., Bokoch, G.M., Traylor-Kaplan, A., Jenkins, G.H., Anderson, R.A., and Schwartz, M.A. (1996). Physical association of small GTPase Rho with a 68kDa phosphatidylinositol 4-phosphate 5-kinase in Swiss 3T3 cells. Mol. Biol. Cell. *7* , 435–442.

Rickert, R.C., Rajewsky, K., and Roes, J. (1995). Impairment of T cell-dependent B-cell responses and B-1 cell development in CD19-deficient mice. Nature *376*, 352–355.

Sato, S., Steeber, D.A., and Tedder, T.F. (1995). The CD19 signal transduction molecule is a response regulator of B lymphocyte differentiation. Proc. Natl. Acad. Sci. USA *92*, 11558–11562.

Sato, S., Jansen, P.J., and Tedder, T.F. (1997). CD19 and CD22 expression reciprocally regulates tyrosine phosphorylation of Vav protein during B lymphocyte signaling. Proc. Natl. Acad. Sci. USA *94*, 13158–13162.

Schuebel, K.E., Bustelo, X.R., Nielsen, D.A., Song, B.J., Barbacid, M., Goldman, D., and Lee, I.J. (1996). Isolation and characterization of murine vav2, a member of the vav family of proto-oncogenes. Oncogene *13*, 363–371.

Songyang, Z., Shoelson, S.E., McGlade J., Oliver, P., Pawson T., Bustelo, X.R., Barbacid M., Sabe, H., Yi, T., Ren, R., et al. (1994). Specific motifs recognised by the SH2 domains of Csk, 3BP2, fps/fes, Grb2, HCP, SHC, Syk and Vav. Mol. Cell. Biol. *14*, 2777–2785.

Stephens, L., Jackson, T.R., and Hawkins, P.T. (1993). Activation of phosphatidylinositol 4,5-bisphosphate supply by agonists and non-hydrolysable GTP analogues. Biochem. J. *296*, 481–488.

Tarakhovsky, A., Turner, M., Schaal, S., Mee, P.J., Duddy, L.P., Rajewsky, K., and Tybulewicz, V.L. (1995). Defective antigen receptor-mediated proliferation of B and T cells in the absence of Vav. Nature *374*, 467–470.

Tedder, T.F., and Isaacs, C.M. (1989). Isolation of cDNAs encoding the CD19 antigen of human and mouse B lymphocytes: a new member of the immunoglobulin superfamily. J. Immunol. *143*, 712–717.

Tolias, K.F., Cantley, L.C., and Carpenter, C.L. (1995). Rho family GTPases bind to phosphoinositide kinases. J. Biol. Chem. *270*, 17656–17659.

Tooze, R.M., Doody, G.M., and Fearon, D.T. (1997). Counterregulation by coreceptors CD19 and CD22 of MAP kinase activation by membrane immunoglobulin. Immunity *7*, 59–67.

Turner, M., Mee, J.P., Walters, A.E., Quinn, M.E., Mellor, A.L., Zamoyska, R., and Tybulewicz, V.L.J. (1997). A requirement for Rho-family GTP exchange factor Vav in positive and negative selecton of thymocytes. Immunity *7*, 451–460.

Tuveson, D.A., Carter, R.H., Soltoff, S.P., and Fearon, D.T. (1993). CD19 of B cells as a surrogate kinase insert region to bind phosphatidylinositol 3-kinase. Science *260*, 986–989.

Weng, W.K., Jarvis, L., and LeBien, T.W. (1994). Signaling through CD19 activates Vav/mitogen-activated protein kinase pathway and induces formation of a CD19/Vav/phosphatidylinositol 3-kinase complex in human B cell precursors. J. Biol. Chem. *269*, 32514–32521.

Woscholski, R., Waterfield, M.D., and Parker, P. (1995). Purification and biochemical characterization of the mammalian phosphatidylinositol 3,4,5-triphosphate 5-phosphatase. J. Biol. Chem. *270*, 31001–31007.

Wu, J., Motto, D.G., Koretzky, G.A., and Weiss, A. (1996). Vav and SLP-76 interact and functionally cooperate in IL-2 gene activation. Immunity *4*, 593–602.

Yamamoto, M., Marui, N., Sakai, T., Morii, N., Kozaki, S., Ikai, K., Imamura, S., and Narumiya, S. (1993). ADP-ribosylation of rhoA gene product by botulinum C3 exoenzyme causes Swiss 3T3 cells to accumulate in the G1 phase of the cell cycle. Oncogene *8*, 1449–1455.

Zhang, R., Alt, F.W., Davidson, L., Orkin, S.H., and Swat, W. (1995). Defective signalling through the T- and B-cell antigen receptors in lymphoid cells lacking the vav proto-oncogene. Nature *374*, 470–473.